ARTICLE

Nanocontact Electrification through Forced Delamination of Dielectric Interfaces

Jesse J. Cole, Chad R. Barry, Xinyu Wang, and Heiko O. Jacobs*

Department of Electrical and Computer Engineering, University of Minnesota, 200 Union Street SE, Minneapolis, Minnesota 55455, United States

ABSTRACT This article reports patterned transfer of charge between conformal material interfaces through a concept referred to as nanocontact electrification. Nanocontacts of different size and shape are formed between surface-functionalized polydimethylsiloxane (PDMS) stamps and other dielectric materials (PMMA, SiO_2). Forced delamination and cleavage of the interface yields a well-defined charge pattern with a minimal feature size of 100 nm. The process produces charged surfaces and associated fields that exceed the breakdown strength of air, leading to strong long-range adhesive forces and force—distance curves, which are recorded over macroscopic distances. The process is applied to fabricate charge-patterned surfaces for nanoxerography demonstrating 200 nm resolution nanoparticle prints and applied to thin film electronics where the patterned charges are used to shift the threshold voltages of underlying transistors.

KEYWORDS: nanocontact electrification · transfer printing · nanoxerography · flexible printable electronics · charge patterning

Charge transfer upon contact between the surfaces of two electrically neutral materials through contact electrification is a well-known phenomenon that can be attributed to three fundamental processes: transfer of electrons, ions, or charged material. Contact electrification leads to uncompensated surface charges that significantly impact the force of adhesion. These forces can be very large. Measurements using point contacts between crossed cylinders recorded record levels where the electrostatic forces exceeded 6 J per m^2, which is in the range of fracture energies for covalently bonded materials.[1] Considering the context of soft lithography,[2] nanoimprint lithography, and nanotransfer printing,[3] the formation and fracture of conformal contacts have become mainstream and are no longer limited to single point contacts between crossed cylinders. Many techniques currently exist for the patterning of charges on a surface including direct writing[4] charges by AFM, parallel patterning[5] by contact with a thin flexible gold electrode, exposure to electron[6] and ion[7] beams, applying the photovoltaic[8] effect, and jet printing[9] of a charged solvent. The applications for these charged surfaces have been directed primarily toward the assembly of oppositely charged nanoparticles from the gas and liquid phases. When immobilized in a predetermined location, nanoparticles could form the building blocks of next generation nanoelectronic devices that take advantage of nanoparticle properties including high crystallinity and large surface area. This motivates a new set of investigations into the fundamental science and applications of contact electrification at these interfaces over extended surfaces using multiple contacts of different size and shape.

This article reports a first set of experiments and results of high levels of contact electrification which occurs between poly(dimethylsiloxane) (PDMS) stamps that are brought in contact with silicon dioxide (SiO_2) and poly(methyl methacrylate) (PMMA). The experiments yield charged surfaces and associated fields that exceed the breakdown strength of air leading to strong long-range adhesive forces. Proton exchange reactions established in solution chemistry are proposed to explain the observed interfacial charging. The process finds several applications. It is applied to the printing of charge, printing of nanoparticles, and charge-based doping to shift the threshold voltage of thin film transistors. Regarding the charge patterning application, the chemically driven process eliminates the need for prior[5,10−12] conducting electrodes and external voltages to deliver and pattern charge. The charge patterns attract nanoparticles and support ~100 nm resolution prints containing <50 nm Ag particles. Finally, in the context of printable

*Address correspondence to hjacobs@umn.edu.

Received for review July 16, 2010 and accepted October 19, 2010.

Published online October 25, 2010. 10.1021/nn1016692

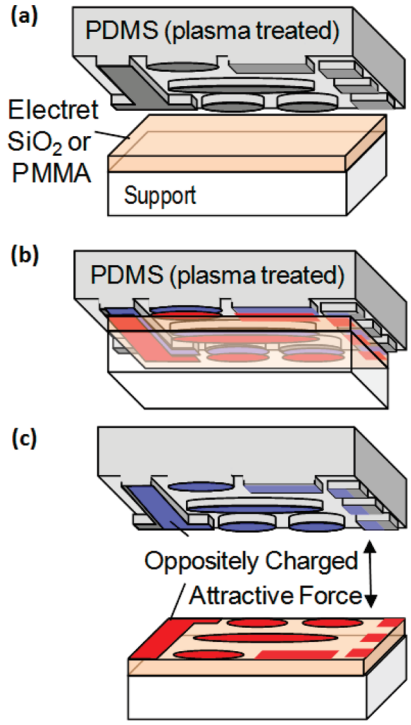

Figure 1. Contact electrification process. (a) Dielectric coated substrate is placed in contact with an oxygen plasma treated, patterned PDMS stamp. (b) Charge transfer occurs at the areas of contact between both materials and leads to an increase in short-range adhesion. (c) Forced delamination yields oppositely charged surfaces and long-range attractive force.

electronics, it is demonstrated that a contact with PDMS leads to high levels of uncompensated surface charge which affects transport in nearby semiconducting device layers which is measured in terms of transistor threshold voltage shifts, which exceeded 500 mV in the MOSFET devices that have been tested.

RESULTS AND DISCUSSION

Figure 1 illustrates the nanocontact electrification process between insulating surfaces. PDMS was chosen as the primary contacting material and was either patterned in topography through molding[5,10] to provide small contact areas surrounded by unchanged surface areas or it was left flat to lay down a uniform layer of charge. To clean and activate the PDMS surface (Figure 1a), we used a pure oxygen plasma etcher (SPI Plasma Prep II) operating at 80−100 W at 10 Torr for 40 s. This process is used because it creates an energetic, hydrophilic surface that reduces transfer of uncured material during contact when compared to untreated PDMS.[13−16] Untreated PDMS did not result in high levels of charge transfer. As electrets, we tested PMMA and SiO_2. The PMMA was spin-coated and baked according to standard procedures to produce a film thickness of 200 nm. The SiO_2 layer was a 160 nm thick and was generated by dry thermal oxidation. The nanocontact electrification process involves bringing the two dielectric surfaces in conformal contact (Figure 1b),

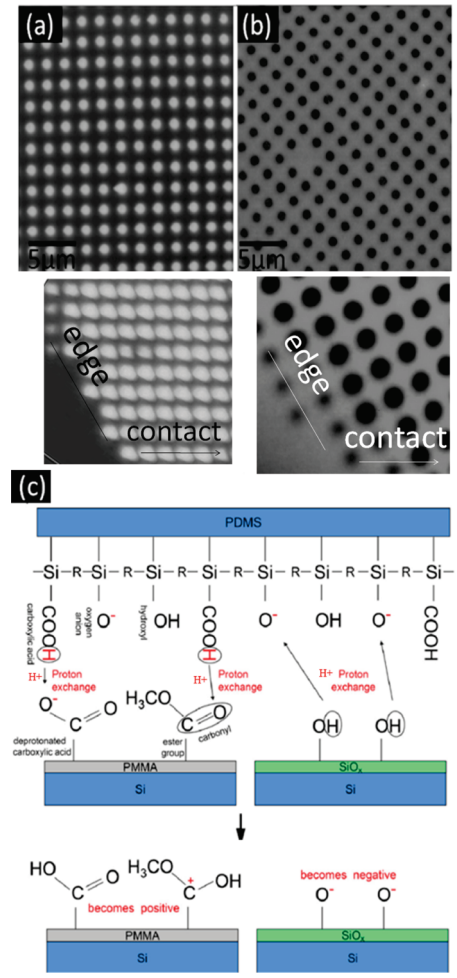

Figure 2. KFM contact electrification results and charge transfer theory. (a,b) KFM images of 1 μm pitched dot patterns showing the influence of material on the polarity. (a) PMMA charged positively and (b) SiO_2 charged negatively upon contact with the same plasma activated PDMS stamp. The edge of the stamp-contacted region was recorded to determine the extent of lateral charge diffusion. (c) Proposed proton exchange reaction. In the case of PMMA, hydrogen protons dissociate from the PDMS surface and attach to a deprotonated carboxylic acid or carbonyl site within the ester groups on the PMMA surface. The situation is reversed for SiO_2 due to the abundance of hydroxyl groups on the SiO_2 surface.

leaving the surface in contact to react for 1 min, and delamination. The delamination process (Figure 1c) yields oppositely charged surface patterns on each side, which are characterized using Kelvin probe force microscopy (KFM).[17] In addition to the KFM measurements, we used a balance to record long-range electrostatic attraction as a function of separation. The balance (Ohaus Adventurer) was used in combination with a micromanipulator to record force−distance curves described later. In the force measurement experiments, the contacting structure is mounted onto the plate of a microbalance, which records a weight reduction after forced delamination.

Figure 2 depicts the KFM images of (a) PMMA *versus* (b) SiO_2 surfaces after being brought in contact

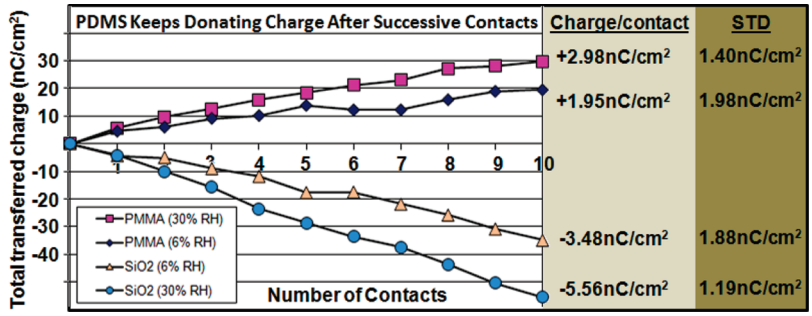

Figure 3. Cumulative donated charge from a single piece of PDMS to PMMA and SiO_2 at 6 and 30% relative humidity. Repeated contact to fresh PMMA and SiO_2 surfaces resulted in continued charge transfer. The average charge per contact and standard deviation per contact are displayed next to their respective lines.

with PDMS and our hypothesis of the charging mechanism. Experimentally, we find that PMMA charged positively at contacted areas, while SiO_2 charged negatively. Localized electrification is observed after conformal contacts are delaminated. The edge of the stamp-contacted region was recorded as well since it is an area where the periodic potential is disturbed. Even this region shows minimal lateral charge diffusion; however, no charge patterns are observed in regions where the PDMS did not contact. The uncontacted substrate areas serve as control areas for reference to the charge patterns in the contacted areas. The recorded potential difference in KFM studies can be used as a first-order estimate of the trapped surface charge density. In the illustrated example, we recorded +250 mV potential difference for the 200 nm thick PMMA film, which represents a charge density of 3.25 nC/cm^2 and −300 mV for the 160 nm thick SiO_2 film which represents 7.3 nC/cm^2.[18] The charging could, in principle, be attributed to a number of factors including material transfer. To determine if material transfer played an important role, we conducted several atomic force microscopy (AFM) and X-ray photon spectroscopy (XPS) studies (shown in Supporting Information Figure S1). We found no measurable material transfer between plasma treated PDMS and untreated PMMA, which is consistent with prior XPS studies by others.[13−16] Yet PMMA charges highly upon contact, as shown in Supporting Information Figure S2. In the case of SiO_2, things are more complicated and are more sensitive to the details of oxygen plasma treatment. We tested two types of plasmas with different oxygen concentrations and pressure. Specifically, a 1 min 100% oxygen plasma treatment at 100 mTorr, which is used for etching (STS RIE etcher), was found to lead to covalent bonding between the PDMS and SiO_2 with a detectable amount of PDMS transferred upon forced delamination. Yet these PDMS stamps did not provide the highest level of charge and could not be used repeatedly. In contrast at 10 Torr, air-based 20% oxygen plasma treatment (SPI Plasma Prep II) for the same time allowed delamination of the PDMS from SiO_2, producing high charge levels and low material transfer. The latter PDMS stamps could be used multiple times to charge a surface, as will be discussed in Figure 3. The lack of correlation between charge and material transfer combined with the ability to support successive charging leads to the conclusion that material transfer is not the dominant charging mechanism.

The working hypothesis for the charging mechanism is illustrated in Figure 2c and involves hydrogen proton exchange at the interface. It is known that plasma treatment attacks the Si-CH_3 bonds on the surface of the PDMS, leaving very reactive silyl radicals that capture O, OH, COOH, and oxygen radicals, forming a mildly acidic and highly polar surface.[13,15] PMMA on the other hand can be considered as being "less acidic" than plasma treated PDMS because it contains fewer surface hydrogen atoms. This creates a chemical potential difference that allows hydrogen protons to transfer during contact. After separation, the hydrogen atoms remain trapped on the PMMA surface, leaving these areas positively charged. In accordance with this hydrogen proton exchange reaction theory, silicon dioxide was tested as it should yield the opposite polarity since the oxidized surface of the SiO_2 substrate has an abundance of hydroxyl groups making it "more acidic" than PDMS.

In terms of the degradation of the charging ability of the PDMS as a function of use, we found that plasma activated PDMS can be used multiple times before it needs reactivation; no measurable degradation was observed after 10 charging experiments. This observation can be explained if we compare the estimated surface charge densities (3−7 nC/cm^2) with the intermolecular spacing of the reactive sites that are available. The 7 nC/cm^2 is a high level of charge which appears to be self-limited by the dielectric breakdown strength of air, as will be discussed below. From a molecular standpoint, however, 7 nC/cm^2 is only one elementary charge per 40 nm × 40 nm sized area. For example, the area per silanol group is estimated to be 0.7 nm × 0.7 nm. This leads to an abundance of surface groups on the PDMS that can continue to take part in the reaction. The large quantity of surface groups supports the observation that the PDMS can be used as a charge source multiple times.

Figure 3 plots the resulting amount of charge that was donated by a single piece of PDMS over successive contacts. The amount of charge that is donated in each step can be monitored by placing each freshly charged sample on a Faraday cup. The Faraday cup is connected to a Keithley 6517A electrometer that records the induced image charge which provides a direct measure of how much charge has been donated to the two dielectrics, PMMA or SiO_2. Each time, the same piece of PDMS contacted a fresh dielectric surface. The figure shows PMMA in the upper half and SiO_2 in the lower half. The results show that increasing the humidity from 6 to 30% increased the amount of overall charge transferred. It has previously been reported that water plays an important role in triboelectric charging of toner particles and polymers,[19−21] where faster charging was observed[22] at higher relative humidity. A similar trend was observed in a more recent and unrelated study that reported that surface can be charged through gas-surface reactions. The authors changed the relative humidity[23,24] and found higher levels of uncompensated surface charge at raised humidity. In our case, the increased charge levels could be explained by the polymeric amorphous and hydrophilic structure of oxygen plasma treated PDMS, which leads to a greater uptake of water and ionic species to participate in the ion transfer.

Using the KFM-based estimated 3−7 nC/cm^2 of uncompensated surface charge, we can evaluate the resulting electric field, $E = \sigma/\varepsilon_0$, where σ is the surface charge density, and ε_0 is the permittivity of air gap that is formed. The estimated values for the electric field are 3.5×10^6 V/m for PMMA and 8×10^6 V/m for SiO_2, which exceeds the dielectric breakdown strength of air ($\sim 3 \times 10^6$ V/m) published for macroscopic electrodes. The closeness of these values to the theoretical limit raises the issue if the observed charge levels are limited or self-regulated by dielectric breakdown strength of air. In principle, it could be possible that electrostatic discharge takes place during charge separation, which limits the charge level to the reported values. Short-range discharge phenomena between separating surfaces have been reported by Horn *et al.*[1] using surface force apparatus measurements; the observed abrupt reductions in the Coulomb attraction were attributed to a stepwise reduction in the remaining uncompensated charges. These types of discharges occur over short distances and may therefore not be accompanied with light flashes and popping sounds that can be detected by simple observation. While discharges may be present and self-limiting, they did not result in localized pockets where complete neutralization took place.

A consequence of separated charges at the interface will be an attractive force which can be estimated using $F/A = \sigma^2/2\varepsilon_0$, where A is the contact area. The estimated electrostatic attraction based in KFM data exceeds 100 N/m^2, suggesting that the charged surface could lift $\sim$9 kg/m^2. To directly measure this estimated attraction, we mounted the contacting structure on a balance that monitors the produced lift force after separation. Figure 4a shows the force−distance curves that were measured by recording the weight reduction as a function of separation for SiO_2 substrates after contact with untreated and oxygen plasma treated PDMS. The reference is untreated PDMS, which provides low levels of contact electrification and low Coulomb attraction. The left side of the graph plots the overall adhesive force before separation occurs (no airgap, short-range force scale to the left). The right side of the graph plots the attractive Coulomb force as the substrates reap-

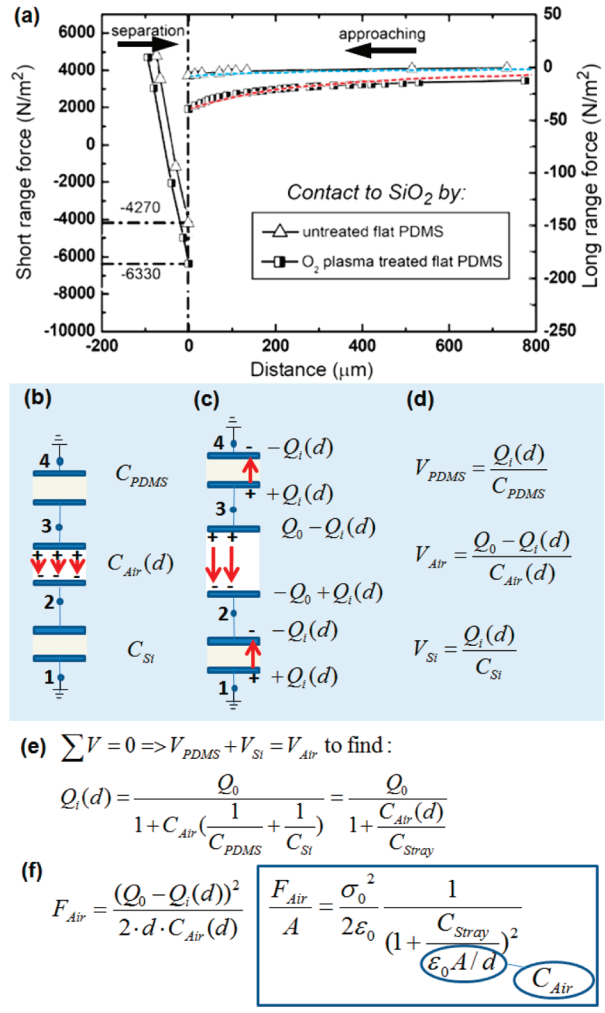

Figure 4. (a) The right side depicts the recorded long-range Coulomb attractive force as a function of separation which is fit to a stray capacitance model (dashed lines) that accounts for induced image charges in nearby conductors. (b,c) As the two surfaces are separated $C_{Air}(d)$ is reduced and the field distribution changes to involve the stray capacitance to nearby grounded surfaces, resulting in a separation-dependent electric field and potential distribution. (d-f) Provides the mathematical steps to derive the force distance curve in the given case where the PDMS was mounted onto a grounded copper plate and the electret was a spin coated layer on a grounded Si substrate.

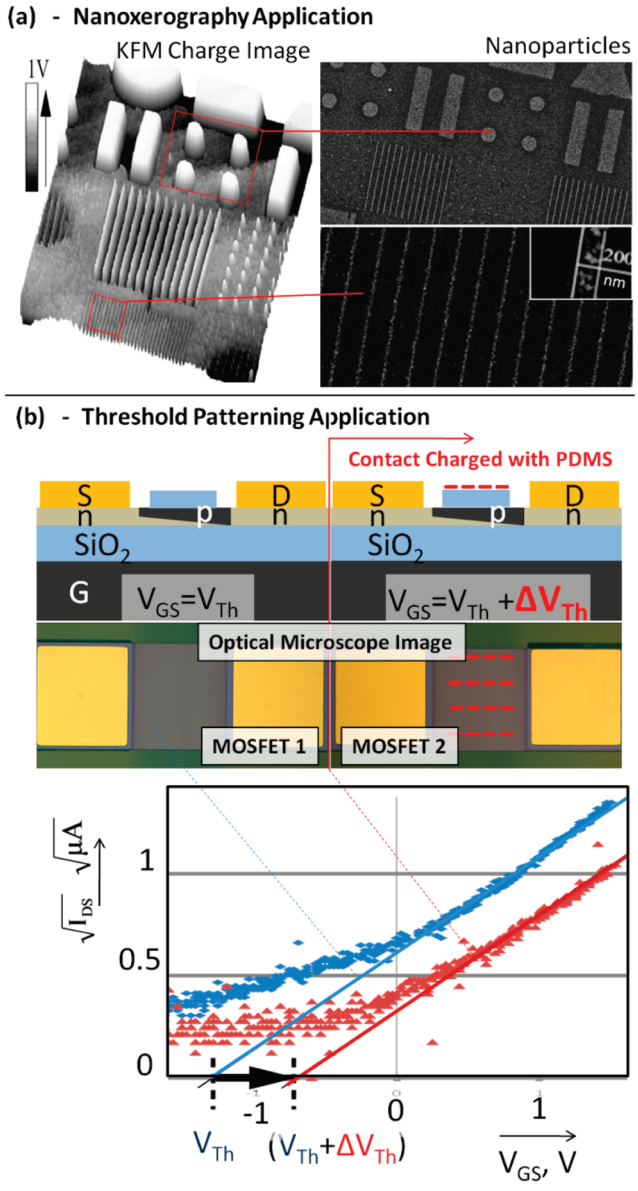

Figure 5. Applications of contact electrification in nanoxerography and thin film electronics. (a) KFM charge images and corresponding 200 nm resolution nanoxerography nanoparticle prints. (b) Thin film electronics application showing schematic, optical microscope image, and $\sqrt{I_{DS}}$ *vs* V_{GS} plot of charge-patterned MOSFETs achieving a threshold voltage shift of 580 mV.

proach the previously contacted PDMS surfaces (with airgap, long-range force scale to the right). The required force to pull the two plane-parallel surfaces apart (left) is typically 2 orders of magnitude larger than the maximum long-range attractive force with an airgap in place (right). At present, the long-range attractive force across an airgap reaches 50 N/m^2 before the two surfaces snap into contact. This is the highest possible data point we have recorded so far. The last data point is difficult to record as it depends on how parallel the surfaces are when they reapproach each other, which may also explain the discrepancy between this ~50 N/m^2 value and the KFM-based estimate which predicted >100 N/m^2. However, both KFM and direct force measurements confirm that the values for the charge density, electric field, and forces are near the theoretical limit set by the dielectric breakdown of air.

In our force−distance measurements, the PDMS and electret surfaces were mounted on grounded copper plates, as depicted schematically in Figure 4b, which act as Faraday cups that provide the ability to monitor image charges. Image charges are a direct result of stray capacitances to nearby conductors and dielectric materials that surround the charged layers. Figure 4c shows that any stray capacitance will reduce the measured long-range force of adhesion as the separation is increased. In other words, the force is not constant as suggested by the previously discussed equation where the force density $F/A = \sigma^2/2\varepsilon_0$ is independent of separation d. A more accurate model for the force−distance curves can be found following Figure 4d,e. The result is shown in Figure 4f using $F/A = \sigma^2/2\varepsilon_0 \times 1/(1 + C_{stray}/[\varepsilon_0 A/d])^2$, where C_{stray} is related to stray capacitance of the charged surfaces to both grounded copper plates. The model is derived by applying the integral form of Gauss' law around the top and bottom electrodes followed by superposition of the respective electric fields. For the $d = 0$ limit case, the force reduces to the equation $F/A = \sigma^2/2\varepsilon_0$ discussed earlier to estimate transferred charge densities, and the image charges in the nearby copper mounting plates are negligible.

Figure 5 discusses applications of uncompensated surface charges. Figure 5a shows an application where the recorded charge pattern (left, KFM image) is used to attract nanoparticles (right, SEM image). In the given example, <50 nm sized negatively charged silver particles were deposited directly from the gas phase using a previously reported nanomaterial source.[10,11] The image demonstrates that the field is strong enough to attract the particles to the charged areas with 200 nm resolution.

Figure 5b shows that contact electrification can also be used to alter electronic transport in nearby semiconducting device layers. In the demonstrated application, patterning of charge is used to alter the threshold voltage of thin film Si transistors from one area to another. Figure 5b shows a device schematic before (left) and after contact (right); full fabrication details are described in the Methods section. The I_{DS} *versus* V_{GS} transistor curves shown were taken using the handle wafer as a back gate. We used the *x*-axis intercept of $\sqrt{I_{DS}}$ *versus* V_{GS} line to evaluate the threshold voltage.[25] For SiO_2, the threshold voltage applied to the back gate shifts to a 580 mV higher voltage, which is consistent with the expected presence of negative surface charge on the SiO_2 surface.

CONCLUSION

In conclusion, the cleavage of conformal contacts, which has become a common procedure in areas of soft-lithography and other soft-printing processes, typically leaves behind large amounts of surface charge as the surfaces are delaminated. While these surface charges remain undetected with most commonly applied spectroscopic measurement techniques including XPS and FTIR, direct evidence can be gained through Kelvin probe force microscopy and force−distance curve measurements. The recorded charging levels can be very high, and the upper levels seem to be self-limited by the dielectric breakdown strength of air. The separated charges give rise to an electrostatic force of adhesion that can be detected over millimeter distances, exceeding 50 N/m^2 in some cases. The corresponding force−distance curves depict a phenomenological relationship between short- and long-range attractive forces. The presented explanation suggests a two-step process whereby the formation and delamination of interfaces bonded by ions precedes contact electrification and the generation of long-range electrostatic forces. SiO_2 and PMMA are commonly used in the processing of semiconductor devices. We therefore expect that our findings will impact areas which go beyond the demonstrated charge-directed assembly and transfer applications. Specifically, the emerging field of printable and flexible electronics could be impacted, where contact printing methods and delamination of interfaces are used to print and transfer materials. We anticipate that the presence of high levels of uncompensated charges may alter the functionality of various electronic devices including FETs unless models take these extra gate charges into account. The additional challenges are particularly relevant in the context of flexible electronics where thin semiconductors, polymer insulators, and conformal contacts are widely employed.

METHODS

PDMS Fabrication and Surface Treatments: PDMS fabrication for this study was unaltered from the commonly accepted technique. Specifically, we mixed 30 g of elastomer (Sylgard 184) and 3 g of curing agent (also Sylgard 184) together for about 2 min at room temperature. Mixing caused gas bubbles to form, so uncured PDMS was degassed in a vacuum chamber at ~30 Torr for 20 min. The uncured PDMS was poured onto silanized silicon, then degassed again for 1 h at ~20 Torr. (The silicon may also be patterned with S1813 photoresist prior to treatment with octadecyltrichlorosilane if features were desired for the finished PDMS.) The degassed PDMS is cured in a convection oven at 60 °C for 12 h. The cured PDMS was inserted into a commercially available plasma cleaner (SPI, model Plasma Prep II) for oxygen plasma treatment. The system was purged with 99.99% oxygen, then the 80−100 W 13.56 MHz RF plasma was operated at 10 Torr for 40 s.

Thin-SOI MOSFET Fabrication: Fabricating the charge-sensitive thin-SOI MOSFETs involved n-well doping, mesa etching, contact deposition, annealing, and insulator deposition. Each step used a pattern and etch-back process to avoid any debris that may be caused by liftoff processes. Beginning with 150 mm diameter p-type Si on insulator wafers (SOITEC, inc.) with a 100 nm Si device layer on a 200 nm buried oxide, we deposited 300 nm SiO_2 by PECVD at 340 °C. To define the dopant mask, S1805 photoresist was photolithographically patterned then given a 30 s oxygen plasma descum, and the underlying SiO_2 was etched in 10:1 buffered oxide etch (a mix of HF and NH_4F in H_2O) for 150 s. The photoresist was removed by rinsing with acetone, methanol, and isopropyl alcohol. Phosphorus containing n-type spin-on dopant was spun on the wafer and then driven in by rapid thermal annealing at 900 °C for 10 s under 6 sLpm flow of 10% oxygen in nitrogen. The oxidized spin-on dopant was stripped in 49% HF for 120 s. The sample was coated with 50 nm SiO_2 by PECVD at 340 °C to prevent metal from contacting p-Si, then windows to the n-wells were opened in the SiO_2 by photolithography, 30 s oxygen plasma descum, and etching 30 s in 10:1 BOE. Photolithography and oxygen descum were used to define ribbons of p-n-p silicon, then 10:1 BOE removed the oxide; a 30 s 20 W 40 mTorr $SF_6/Ar/O_2$ plasma etch removed silicon down to the buried oxide, and the photoresist was removed. Metal contacts were deposited by DC sputtering using a quartz crystal monitor to measure the film thicknesses. Both top(source/drain) and back(gate) contacts were 150 nm Au with a 5 nm Cr adhesion layer. The contacts were patterned by photolithography, oxygen plasma descum, etching 25 min in 10:1 DI H_2O/GE-6 gold etchant and a 60 s dip in 4:1 DI H_2O/CR-12S chrome etchant. The contacts were annealed by RTA at 400 °C for 20 s in 8 sLpm forming gas (5%H_2/95%N_2).

Acknowledgment. This research was partially supported by NSF CMMI-0755995 and CMMI-0621137.

Note Added after ASAP Publication: This article was published on October 25, 2010. The caption to Figure 4 and the Conclusion paragraph have been updated. The corrected version was reposted on November 10, 2010.

Supporting Information Available: XPS study of material transfer, AFM topography of contacted samples with corresponding KFM charge images. This material is available free of charge *via* the Internet at http://pubs.acs.org.

REFERENCES AND NOTES

1. Horn, R.; Smith, D.; Grabbe, A. Contact Electrification Induced by Monolayer Modification of a Surface and Relation to Acid−Base Interactions. *Nature* **1993**, *366*, 442–443.
2. Xia, Y.; Whitesides, G. Soft Lithography. *Annu. Rev. Mater. Sci.* **1998**, *28*, 153–184.
3. Loo, Y.; Willett, R.; Baldwin, K.; Rogers, J. Interfacial Chemistries for Nanoscale Transfer Printing. *J. Am. Chem. Soc.* **2002**, *124*, 7654–7655.
4. Mesquida, P.; Stemmer, A. Attaching Silica Nanoparticles from Suspension onto Surface Charge Patterns Generated by a Conductive Atomic Force Microscope Tip. *Adv. Mater.* **2001**, *13*, 1395–1398.
5. Jacobs, H.; Whitesides, G. Submicrometer Patterning of Charge in Thin-Film Electrets. *Science* **2001**, *291*, 1763–1766.
6. Fudouzi, H.; Kobayashi, M.; Shinya, N. Assembling 100 nm Scale Particles by an Electrostatic Potential Field. *J. Nanopart. Res.* **2001**, *3*, 193–200.
7. Fudouzi, H.; Kobayashi, M.; Shinya, N. Site-Controlled Deposition of Microsized Particles Using an Electrostatic Assembly. *Adv. Mater.* **2002**, *14*, 1649–1652.
8. Liang, S.; Chen, M.; Xue, Q.; Liu, Z. Micro-patterning of TiO_2 Thin Films by Photovoltaic Effect on Silicon Substrates. *Thin Solid Films* **2008**, *516*, 3058–3061.

9. Park, J.-U.; Lee, S.; Unarunotai, S.; Sun, Y.; Dunham, S.; Song, T.; Ferreira, P. M.; Alleyene, A. G.; Paik, U.; Rogers, J. A. Nanoscale, Electrified Liquid Jets for High-Resolution Printing of Charge. *Nano Lett.* **2010**, *10*, 584–591.
10. Barry, C.; Steward, M.; Lwin, N.; Jacobs, H. Printing Nanoparticles from the Liquid and Gas Phases Using Nanoxerography. *Nanotechnology* **2003**, *14*, 1057–1063.
11. Barry, C.; Lwin, N.; Zheng, W.; Jacobs, H. Printing Nanoparticle Building Blocks from the Gas-Phase Using Nanoxerography. *Appl. Phys. Lett.* **2003**, *83*, 5527–5529.
12. Barry, C.; Gu, J.; Jacobs, H. Charging Process and Coulomb-Force-Directed Printing of Nanoparticles with Sub-100-nm Lateral Resolution. *Nano Lett.* **2005**, *5*, 2078–2084.
13. Youn, B.; Huh, C. Surface Analysis of Plasma-Treated Polydimethylsiloxane by X-ray Photoelectron Spectroscopy and Surface Voltage Decay. *Surf. Interface Anal.* **2003**, *35*, 445–449.
14. Kim, H.; Cho, Y.; Lee, H.; Kim, S.; Ryu, S.; Kim, D.; Kang, T.; Chung, K. High-Brightness Light Emitting Diodes Using Dislocation-Free Indium Gallium Nitride/Gallium Nitride Multiquantum-Well Nanorod Arrays. *Nano Lett.* **2004**, *4*, 1059–1062.
15. Bhattacharya, S.; Datta, A.; Berg, J.; Gangopadhyay, S. Studies on Surface Wettability of Poly(dimethyl)siloxane (PDMS) and Glass under Oxygen-Plasma Treatment and Correlation with Bond Strength. *J. Microelectromech. S* **2005**, *14*, 590–597.
16. Langowski, B.; Uhrich, K. Oxygen Plasma-Treatment Effects on Si Transfer. *Langmuir* **2005**, *21*, 6366–6372.
17. Jacobs, H.; Knapp, H.; Muller, S.; Stemmer, A. Surface Potential Mapping: A Qualitative Material Contrast in SPM. *Ultramicroscopy* **1997**, *69*, 39–49.
18. For a double layer separated by a distinct distance d, the charge density σ can be calculated with $\sigma = \varepsilon(\Delta V/d)$, where ε is the permittivity, and ΔV is the voltage drop across the layer. For $\varepsilon = 2 \times 10^{-11}$ C/Vm (relative permittivity of PMMA), $\Delta V = 2$ V (measured potential change), and $d = 200$ nm (assumed intermediate distance between the counter charges), we obtain a first-order estimate of the effective charge density of $\sigma_{eff} = 12.5$ elementary charges per surface area of 100 nm $\times$ 100 nm. The exact number depends on the actual distribution of the charges on the PMMA film and the Si substrate.
19. Nomura, T.; Satoh, T.; Masuda, H. The Environment Humidity Effect on the Tribo-Charge of Powder. *Powder Technol.* **2003**, *135−136*, 43–49.
20. Nemeth, E.; Albrecht, V.; Schubert, G.; Simon, F. Polymer Tribo-Electric Charging: Dependence on Thermodynamic Surface Properties and Relative Humidity. *J. Electrostatics* **2003**, *58*, 3–16.
21. Albrecht, V.; Janke, A.; Nemeth, E.; Spange, S.; Schubert, G.; Simon, F. Some Aspects of the Polymers' Electrostatic Charging Effects. *J. Electrostatics* **2009**, *67*, 7–11.
22. Gouveia, R. F.; Costa, C. A. R.; Galembeck, F. Water Vapor Adsorption Effect on Silica Surface Electrostatic Patterning. *J. Phys. Chem. C* **2008**, *112*, 17193–17199.
23. Gouveia, R. F.; Galembeck, F. Electrostatic Charging of Hydrophilic Particles Due to Water Adsorption. *J. Am. Chem. Soc.* **2009**, *131*, 11381–11386.
24. Ducati, T. R. D.; Simoes, L. H.; Galembeck, F. Charge Partitioning at Gas−Solid Interfaces: Humidity Causes Electricity Buildup on Metals. *Langmuir* **2010**, *26*, 13763–13766.
25. Wainright, S. P.; Hall, S.; Flandre, D. The Effect of Series Resistance on Threshold Voltage Measurement Techniques for Fully Depleted SOI MOSFETs. *Solid-State Electron.* **1996**, *39*, 89–94.